



# Influence of oxophilic behavior of UiO-66(Ce) metal–organic framework with superior catalytic performance in Friedel-Crafts alkylation reaction

Nagarathinam Nagarjun<sup>1</sup> | Patricia Concepcion<sup>2</sup> |  
Amarajothi Dhakshinamoorthy<sup>1</sup>

<sup>1</sup>School of Chemistry, Madurai Kamaraj University, Tamil Nadu, India

<sup>2</sup>Instituto de Tecnología Química CSIV-UPV, Universitat Politècnica de València, Av. De los Naranjos s/n, 46022, Valencia Spain

## Correspondence

Amarajothi Dhakshinamoorthy, School of Chemistry, Madurai Kamaraj University, Tamil Nadu, India.  
Email: admguru@gmail.com

## Funding information

Science and Engineering Research Board, Grant/Award Number: EMR/2016/006500

In recent years, one of the analogous metal organic frameworks (MOFs) with UiO-66(Zr) topology receiving wider attention is UiO-66(Ce), which exhibits interesting properties and high thermal and chemical stability. Hence, in the present work, UiO-66(Ce) is synthesized by adopting an earlier procedure and characterized by series of spectroscopic techniques like UV-visible (UV-Vis), Fourier transform infrared (FT-IR), Raman and scanning electron microscope (SEM) to confirm its structural features and crystallinity using powder X-ray diffraction (XRD) and these results are in close agreement with other reports. The catalytic performance of UiO-66(Ce) was evaluated in the Friedel–Crafts alkylation reaction between  $\beta$ -nitrostyrene and indole to obtain heterocyclic compounds with biological activity. A series of control experiments indicate that  $Ce^{4+}$  located within the framework plays an important role in promoting this reaction and its activity is found to be much superior to that of UiO-66(Zr). This enhanced activity with  $Ce^{4+}$  compared to  $Zr^{4+}$  is attributed due to the higher oxophilicity of  $Ce^{4+}$ , which can readily bind with an oxygen-containing substrate such as  $\beta$ -nitrostyrene. The leaching test confirms the heterogeneity of the reaction and the catalyst can be reused three times with identical activity to the fresh solid. UiO-66(Ce) shows wide substrate scope with high yields of the desired product. A proposed mechanism is also discussed.

## KEYWORDS

heterogeneous catalysis, metal–organic frameworks, solid Lewis acids, UiO-66(Ce), UiO-66(Zr)

## 1 | INTRODUCTION

Metal–organic frameworks (MOFs) are porous solid crystalline materials whose framework is constituted by the arrangement of metal ions or clusters with polytopic organic units through coordination bonds leading to one-, two-, and three-dimensional networks.<sup>[1–3]</sup> One of the unique properties of MOFs compared to other porous solids is their high synthetic flexibility to design different metal clusters and organic linkers, resulting in wide

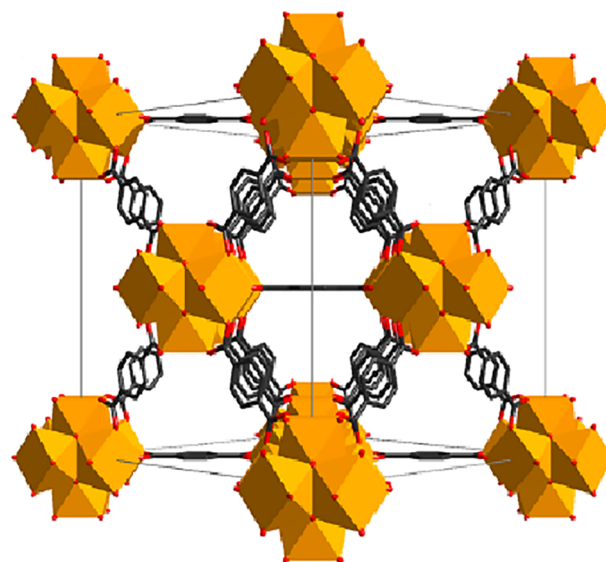
range of topologies of MOFs with attractive physical and chemical properties.<sup>[4]</sup> Porous MOF materials provide notable advantages over other classes of compounds, such as activated carbons, zeolites, and mesoporous silica, in terms of predictable well-defined porosity, surface area, and isolated active sites. The synthetic flexibility and modularity of MOF structures, combined with ultrahigh porosity and surface area, are some of the notable features of MOFs which have been effectively used in many applications, including gas storage,<sup>[5]</sup> gas

separation,<sup>[6]</sup> catalysis,<sup>[7–9]</sup> drug delivery,<sup>[10]</sup> and proton conduction<sup>[11]</sup> among others. In particular, MOFs have been widely reported as solid Lewis acid catalysts for a broad range of reactions.<sup>[12–17]</sup>

In the last two decades, UiO-66(Zr) (UiO: University of Oslo) has been convincingly demonstrated to be one of the most widely studied MOFs for many applications, as listed above, due to its robust chemical stability and easy tunability of active sites in its crystal structure.<sup>[18]</sup> UiO-66(Zr) solid,  $[\text{Zr}_6\text{O}_4(\text{OH})_4(\text{BDC})_6]$  (BDC: 1,4-benzenedicarboxylic acid) was synthesized by the solvothermal method using  $\text{Zr}^{4+}$  as metal ion and BDC as the organic ligand. During the crystal growth of UiO-66(Zr),  $\text{Zr}^{4+}$  cations self-assemble to hexanuclear  $[\text{Zr}_6\text{O}_4(\text{OH})_4]^{12+}$  clusters which are coordinated by BDC ligands to 12 neighboring secondary building units in a face-centered cubic arrangement.<sup>[19,20]</sup> The structural analysis of UiO-66(Zr) exhibits two types of cages with a large octahedral cage (0.9 nm) and a smaller tetrahedral cage (0.7 nm) that can be accessed through triangular windows of about 0.6 nm with the surface area ranging between 1000 and 1500  $\text{m}^2/\text{g}$  depending on preparation methods.<sup>[18]</sup> Furthermore, UiO-66(Zr) exhibits unique features like high thermal, mechanical, and chemical stability and tunable porosity that have facilitated the development of solid catalysts based on UiO-66 for catalytic reactions,<sup>[19]</sup> photocatalytic reactions<sup>[21]</sup> and the influence of defects (missing linker defects) in catalysis.<sup>[22]</sup>

As commented earlier, UiO-66 architecture types of MOFs have been achieved with a wide range of metals ions, such as U(IV),<sup>[23]</sup> Hf(IV),<sup>[24]</sup> Th(IV),<sup>[25]</sup> and Ce(IV).<sup>[26]</sup> UiO-66(Ce) was first reported by Stock and co-workers in 2015 with UiO-66 architecture.<sup>[26]</sup> However, the number of Ce(IV)-based MOFs reported so far is limited, as are their catalytic applications.<sup>[26–32]</sup> The structure of UiO-66(Ce) was obtained by the reaction between cerium(IV) ammonium nitrate (CAN) as the metal ion and BDC as organic linker, leading to the formation of UiO-66(Ce) with UiO-66 type architecture (Figure 1). The crystal structure of UiO-66(Ce) reveals that the clusters  $[\text{Ce}_6\text{O}_4(\text{OH})_4]^{12+}$  are arranged in a cubic close-packed framework and connected by BDC ligands to provide the structural formula  $[\text{Ce}_6\text{O}_4(\text{OH})_4(\text{BDC})_6]$ .<sup>[26]</sup> The Brunauer-Emmett-Teller (BET) surface area of UiO-66(Ce) was reported as 1282  $\text{m}^2/\text{g}$ .

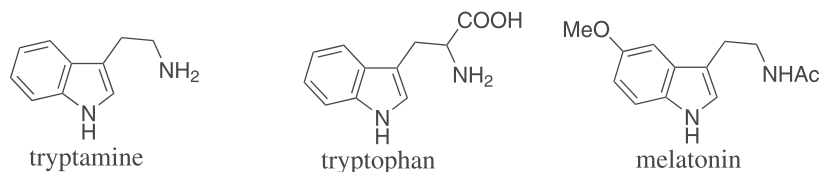
Recently, UiO-66(Ce) has been reported for many applications, such as  $\text{CO}_2$  sorption,<sup>[28]</sup> colorimetric sensing of metal ions,<sup>[33]</sup> CO oxidation,<sup>[34]</sup> and photocatalysis.<sup>[35–39]</sup> However, the catalytic application of UiO-66(Ce) is still in its infancy and the activity of UiO-66(Ce) has been reported to involve synergistic effects.<sup>[40]</sup> Although the number of Ce-based MOFs is limited, they have been reported as acting as redox catalysts in the



**FIGURE 1** Unit cell of compound UiO-66(Ce). Reproduced with permission from ref.<sup>[26]</sup> Copyright Royal Society of Chemistry 2015

aerobic oxidation of benzyl alcohol,<sup>[26]</sup> styrene or cyclohexene,<sup>[29]</sup> and thiol.<sup>[41]</sup> On other hand, homogeneous catalysts containing  $\text{Ce}^{4+}$  as metal ions have been reported for wide range of organic reactions requiring Lewis acids,<sup>[42]</sup> but no Ce-based MOFs have been reported for Lewis acid catalyzed reactions. Bearing these factors in mind, this work describes the preparation and characterization of UiO-66(Ce) using an earlier procedure<sup>[26]</sup> and its catalytic performance is evaluated in the Friedel–Craft alkylation of indole with  $\beta$ -nitrostyrene. Furthermore, this study demonstrates the existence of coordinatively unsaturated sites around  $\text{Ce}^{4+}$  ions in UiO-66(Ce) that allow it to act as a Lewis acid in promoting organic reactions. Some of the other objectives of this work were to develop an environmentally benign, robust catalyst without complicated architecture in the MOF structure for the Friedel–Crafts alkylation reaction between indole and  $\beta$ -nitrostyrene to afford broad ranges of heterocyclic compounds with biologically relevant analogues, and investigate catalyst stability by performing reusability and leaching tests.

The Friedel–Crafts alkylation reaction between indole and  $\beta$ -nitrostyrene is a key organic reaction that is often employed as a preferred route for the production of heterocyclic compounds with biological significance.<sup>[43]</sup> Furthermore, the Friedel–Crafts alkylation reaction is also used as a benchmark reaction to prove the existence of unsaturation around metal centers, especially in solid catalysts possessing Lewis acid sites.<sup>[44,45]</sup> Scheme 1 shows some of the biologically relevant active compounds possessing indole as one of the moieties in their structural skeletons.

**SCHEME 1** Indole containing biologically active compounds

## 2 | EXPERIMENTAL SECTION

### 2.1 | Materials

Ceric ammonium nitrate (CAN),  $\text{ZrOCl}_2 \cdot 8\text{H}_2\text{O}$ ,  $\text{FeCl}_3 \cdot 6\text{H}_2\text{O}$ ,  $\text{Cr}(\text{NO}_3)_3 \cdot 9\text{H}_2\text{O}$ ,  $\text{Co}(\text{NO}_3)_2 \cdot 6\text{H}_2\text{O}$ ,  $\text{Zn}(\text{NO}_3)_2 \cdot 6\text{H}_2\text{O}$ , BDC, 2-methylimidazole, indole derivatives, and  $\beta$ -nitrostyrene were purchased from Sigma Aldrich and used as received without further purification unless otherwise stated. Solvents were also obtained from Sigma Aldrich and used as received without additional purification.

### 2.2 | Instrumentation

Powder X-ray diffraction (XRD) patterns for the solids purchased were measured using a Philips X'Pert diffractometer, United States America with  $\text{CuK}\alpha$  radiation ( $\lambda = 1.5417 \text{ \AA}$ ) in the refraction mode. Fourier transform infrared (FT-IR) spectra were recorded in the region of  $400\text{--}4000 \text{ cm}^{-1}$  with  $2 \text{ cm}^{-1}$  resolution with a Bruker tensor 27 series FT-IR spectrometer, United States. Scanning electron microscopy (SEM) images were collected using a Hitachi S-3000H scanning electron microscope, United Kingdom. UV-visible diffuse reflectance spectroscopy (UV-DRS) spectra were recorded by a Shimadzu UV-2700 ISR-2600 plus instrument, Japan in the range  $200\text{--}800 \text{ nm}$  and the samples were dispersed on the surface of  $\text{BaSO}_4$ . Thermogravimetric analysis (TGA) was carried out in a Netzsch Scientific NJA-STA 2500 Regulus instrument, United Kingdom. Around 3 mg of solid was placed in an  $\text{Al}_2\text{O}_3$  crucible. The TGA profile of the solid was obtained by heating it from ambient temperature to  $800^\circ\text{C}$  with a heating rate of  $10^\circ\text{C}/\text{min}$  under continuous  $\text{N}_2$  flow. Gas chromatography (GC) was employed to determine conversion and selectivity using an Agilent 7820 A model (United States of America) with nitrogen as the carrier gas. Gas chromatography-mass spectrometry (GC-MS), United States of America was used to confirm the products using a 5890 B instrument. The IR spectra of adsorbed CO over UiO-66(Ce) were measured at room temperature using a Nexus 8700 FT-IR spectrometer, United Kingdom with a deuterated triglycine sulfate (DTGS) detector and acquiring at  $4 \text{ cm}^{-1}$  resolution. An IR cell allowing *in situ* measurements in controlled atmospheres with the temperatures from  $-176^\circ\text{C}$  to  $500^\circ\text{C}$  was

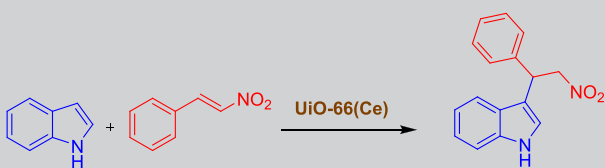
connected to a vacuum system with gas dosing facility. The sample was pressed into self-supported wafers and treated under vacuum ( $10^{-5}$  mbar) at  $150^\circ\text{C}$  for 1.5 hr before IR measurements were made. The sample was cooled to  $-176^\circ\text{C}$  under dynamic vacuum conditions after activation followed by CO dosing at increasing pressure ( $0.1\text{--}1.9$  mbar). IR spectra were measured after introducing each dosage of CO.

### 2.3 | Synthesis of UiO-66(Ce)

UiO-66(Ce) solids were prepared by following a procedure previously reported in the literature.<sup>[26]</sup> Initially, BDC (35.4 mg,  $213 \mu\text{mol}$ ) was placed in a reaction tube followed by the addition of 1.2 ml of *N,N*-dimethylformamide (DMF). To this mixture was added an aqueous solution of CAN ( $400 \mu\text{L}$ ,  $0.5333 \text{ M}$ ). The reaction tube was sealed and placed in a preheated oil bath for 15 min at  $100^\circ\text{C}$  under continuous stirring. The resulting light-yellow precipitate was centrifuged from the mother liquor and washed twice with DMF (2 ml) to remove unreacted BDC from the solids. The obtained solid was washed three times with methanol and centrifuged with methanol (2 ml) to remove DMF. This solid was dried in an air oven at  $80^\circ\text{C}$  to provide UiO-66(Ce) solids.

### 2.4 | General procedure for Friedel–Crafts alkylation between indole and $\beta$ -nitrostyrene

In a typical catalytic reaction, a Schlenk tube was charged with 25 mg of catalyst followed by the addition of indole ( $0.25 \text{ mmol}$ ) and  $\beta$ -nitrostyrene ( $0.25 \text{ mmol}$ ). To this slurry 2 ml of solvent was added and then this heterogeneous reaction mixture was placed in an oil bath maintained at  $80^\circ\text{C}$ . The heterogeneous reaction mixture was stirred for the required time as shown in Table 1. The progress of the reaction was followed by sampling aliquots periodically from the reaction mixture, diluted with acetonitrile and filtered with a syringe filter. These aliquots were analyzed by GC to determine the conversion and selectivity of the resulting product by the internal standard method. After the completion of the reaction, the reaction was quenched and the reaction tube was allowed to cool to

**TABLE 1** Conditions for the Friedel–Crafts alkylation reaction between indole and  $\beta$ -nitrostyrene using UiO-66(Ce) as a solid Lewis acid catalyst<sup>a</sup>


Entry	Catalyst	Temperature (°C)	Solvent	Yield <sup>b</sup> (%)
1	–	80	DCE	–
2	CAN	80	DCE	20
3	BDC	80	DCE	–
4	n-CeO <sub>2</sub>	80	DCE	19
5	UiO-66(Ce)	80	Toluene	71
6	UiO-66(Ce)	60	Chloroform	77
7	UiO-66(Ce)	80	Ethanol	80
8	UiO-66(Ce)	80	Acetonitrile	38
9	UiO-66(Ce)	RT	Dichloromethane	40
10	UiO-66(Ce)	80	DCE	91
11 <sup>c</sup>	UiO-66(Ce)	80	DCE	98 (13) <sup>d</sup>
12	UiO-66(Ce)	70	DCE	63
13	UiO-66(Ce)	60	DCE	50
14 <sup>e</sup>	UiO-66(Ce)	80	DCE	65
15 <sup>f</sup>	UiO-66(Ce)	80	DCE	35
16 <sup>g</sup>	UiO-66(Ce)	80	DCE	5
17 <sup>h</sup>	UiO-66(Ce)	80	DCE	85
18	UiO-66(Zr)	80	DCE	32

Note. RT, room temperature.

<sup>a</sup>Reaction conditions: indole (0.25 mmol),  $\beta$ -nitrostyrene (0.25 mmol), solvent (2 ml), catalyst (25 mg), 24 hr.

<sup>b</sup>Yield was determined by GC.

<sup>c</sup>Indole (0.25 mmol),  $\beta$ -nitrostyrene (0.25 mmol), solvent (0.2 mL), catalyst (25 mg), 24 hr.

<sup>d</sup>Values in parentheses indicate the yield in the absence of catalyst.

<sup>e</sup>Catalyst (15 mg).

<sup>f</sup>Catalyst (5 mg).

<sup>g</sup>Pyridine (20  $\mu$ l).

<sup>h</sup>After third reuse.

room temperature. Later, the mixture was diluted with acetonitrile and filtered and further analyzed by GC to identify the final conversion and selectivity. The products were confirmed by GC-MS and <sup>1</sup>H NMR analyses. An identical procedure was followed to perform control experiments with CAN (39 mg) and CeO<sub>2</sub> nanoparticles (n-CeO<sub>2</sub>) (12 mg) as homogeneous and heterogeneous solid catalysts, respectively, under identical conditions with similar cerium content to UiO-66(Ce).

Reusability tests were performed by following a similar experimental procedure to that described above except

for the addition of recovered catalyst obtained by filtration after the reaction, which was washed three times with fresh acetonitrile (5 ml) and dried at 100°C for 3 hr.

### 3 | RESULT AND DISCUSSION

As noted previously, UiO-66(Ce) was synthesized by the reported procedure<sup>[26]</sup> and the as-synthesized solid was characterized by powder XRD, FT-IR, TGA, UV-DRS, Raman spectroscopy, and SEM analysis to confirm the formation of MOFs as well as to ascertain its structural

integrity and morphology. The powder XRD pattern of UiO-66(Ce) is shown in Figure 2 and clearly demonstrates that the crystalline nature and peak positions of this MOF are in good agreement with the reported diffraction patterns of UiO-66(Ce),<sup>[26]</sup> thus confirming the formation of UiO-66(Ce).

Figure 3 shows SEM images of UiO-66(Ce) and the structural morphology reveals that these MOF crystallites are spherical crystals, which is in close agreement with earlier data.<sup>[26]</sup> The FT-IR spectrum of UiO-66(Ce) is provided in Figure 4 and is also in accordance with earlier reported results.<sup>[26]</sup> Briefly, the asymmetric stretching frequency at  $1560\text{ cm}^{-1}$  and symmetric stretching frequency at  $1384\text{ cm}^{-1}$  are assigned to carboxylate groups in UiO-66(Ce) solid. The Ce–O stretching frequency was expected below  $400\text{ cm}^{-1}$ , but was shifted to  $521\text{ cm}^{-1}$  due to the coordination of BDC linkers with  $\text{Ce}^{4+}$ , which is in agreement with earlier report.<sup>[46]</sup> On other hand, FT-IR spectrum of the  $\text{CeO}_2$  sample did not show any of these characteristic frequencies except a broad band at

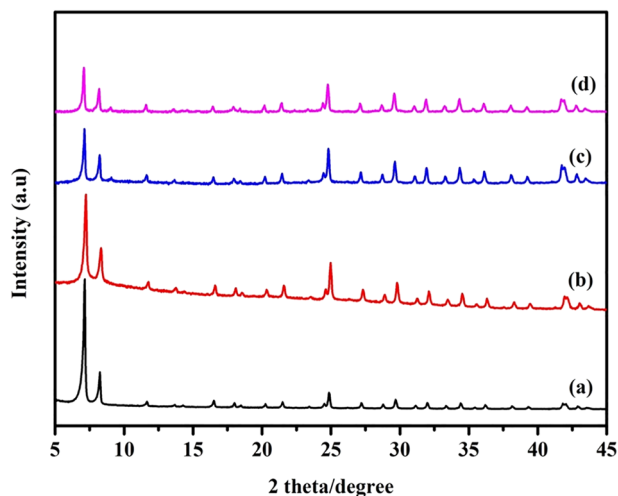


**FIGURE 2** Powder XRD patterns of UiO-66(Ce) (a) fresh, (b) after the reaction, (c) twice reused, and (d) three times reused

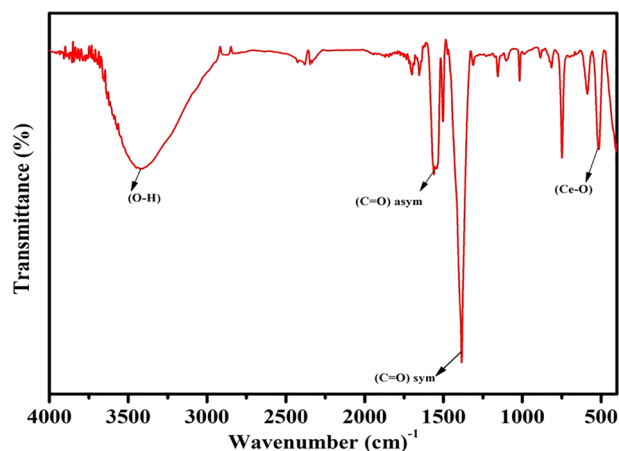


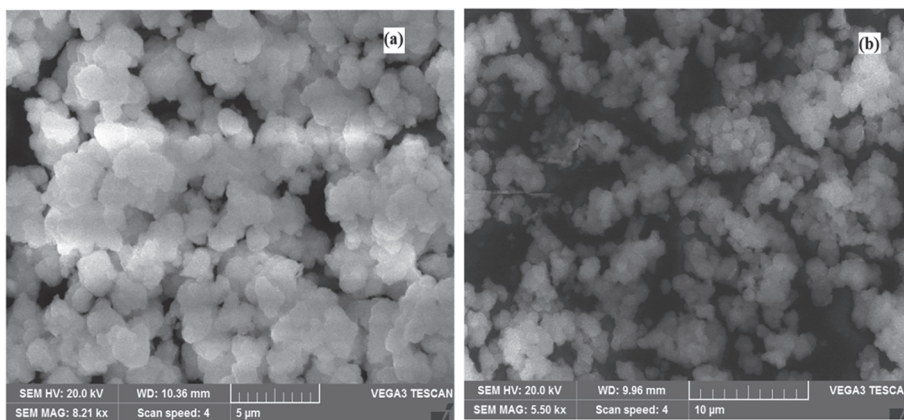
**FIGURE 4** FT-IR spectrum of UiO-66(Ce)

around  $500\text{ cm}^{-1}$  due to Ce–O (Supporting Information Figure S29), thus suggesting the contribution of organic linkers in UiO-66(Ce).

UV-DRS analysis of UiO-66(Ce) was also carried out and the results are given in Figure 5. The absorption edge corresponding to  $\text{Ce}^{4+}$  is observed at around  $400\text{ nm}$ , which agrees well with earlier data reported in literature.<sup>[47]</sup> Furthermore, the absorption bands seen at  $250$  and  $320\text{ nm}$  in the UV region correspond to the charge transfer transition from  $\text{O}^{2-}(2\text{P})$  of BDC linkers to the  $\text{Ce}^{4+}(4\text{f})$  orbital.<sup>[48]</sup> However, the absorption bands below  $400\text{ nm}$  are blue shifted with  $\text{CeO}_2$  solid, suggesting the influence of the chemical environment around  $\text{Ce}^{4+}$  provided by BDC linkers in UiO-66(Ce).

The Raman spectrum of UiO-66(Ce) and its corresponding BDC linker are shown in Figure 6. UiO-66(Ce) solid exhibits a main band at around  $460\text{ cm}^{-1}$  assigned to the vibrational mode<sup>[49]</sup> that clearly confirms the existence of Ce in the tetravalent oxidation state in the framework of UiO-66(Ce). The vibrational bands corresponding to the BDC linker are also shown in Figure 6 and these bands are also seen in UiO-66(Ce). However, the vibrational band for the Ce–O bond is seen

**FIGURE 3** SEM images of UiO-66(Ce) (a) fresh and (b) three times reused



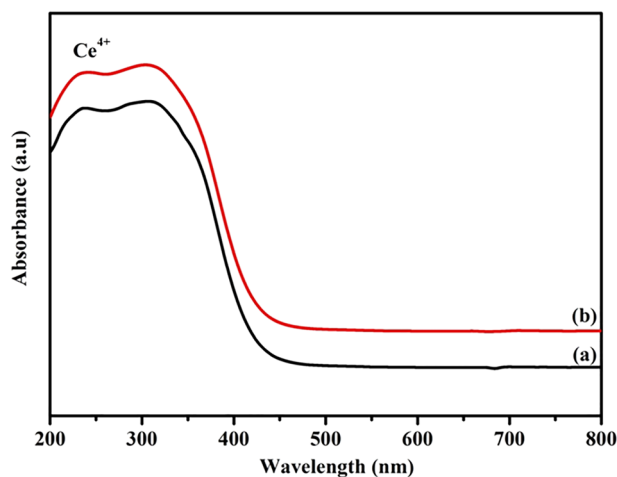


**FIGURE 5** UV-DRS spectra of UiO-66(Ce) (a) fresh and (b) three times reused

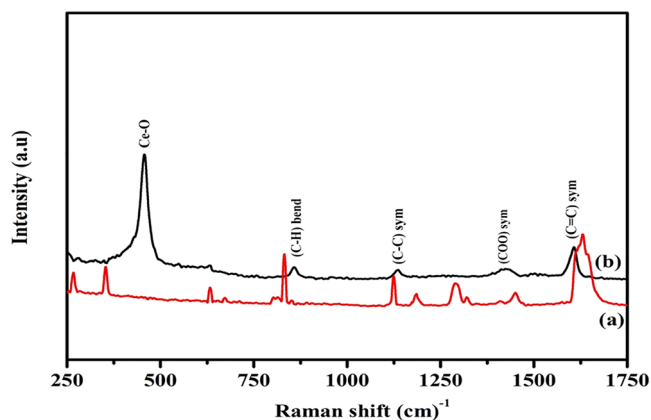


**FIGURE 6** Raman spectra of (a) BDC and (b) UiO-66(Ce)

at a higher intensity in UiO-66(Ce), dominating the other vibrational bands corresponding to the BDC linker but with lower intensity.

TGA of UiO-66(Ce) was also recorded under a nitrogen atmosphere and the observed data are presented in Supporting Information Figure S1. The thermal stability of this MOF collapses above 300°C.<sup>[26]</sup> From the TGA results, it is confirmed that the as-synthesized solid consists of structural defects arising from the missing of BDC linkers connected to metal clusters. The observed TGA results indicate that  $[\text{Ce}_6\text{O}_4(\text{OH})_4]^{12+}$  clusters are coordinated by 11 BDC linkers instead of 12 BDC linkers, as evidenced by a weight loss of 4 wt% lower during the framework collapse than the expected weight loss of 34 wt% for defect-free solid.<sup>[26,50]</sup> Furthermore, UiO-66(Zr) was synthesized by following the reported literature of Lamberti and coworkers.<sup>[51]</sup> The structural defect in UiO-66(Zr) was established by characterizing the solid by TGA. UiO-66(Zr) was found to be stable up to 375°C.

The expected weight loss for the defect-free solid relative to the formation of  $\text{ZrO}_2$  in the last step was 54.6%, but the experimental data exhibited a weight loss of only around 50% (Supporting Information Figure S27).<sup>[51]</sup> Therefore, the as-prepared solid was found to be defective as it exhibited 11 ligands per inorganic  $\text{Zr}_6\text{O}_4(\text{OH})_4$  cluster instead of 12. The observed weight loss at different temperatures is also in close agreement with earlier reported data (Supporting Information Figure S27).<sup>[51]</sup> Zhou and co-workers<sup>[52]</sup> and Lillerud and co-workers<sup>[50]</sup> have determined the missing linker around the  $\text{Zr}_6\text{O}_4(\text{OH})_4$  cluster by TGA. These results indicate that the structural defects in UiO-66(Zr) are very similar to those in UiO-66(Ce).

Figure 7 shows the IR spectra of CO adsorption on the UiO-66(Ce) MOF sample with the presence of bands at 2174, 2153, 2135, and 2125  $\text{cm}^{-1}$ , ascribed to CO bonded to  $\text{Ce}^{4+}$ , CO hydrogen bonded with hydroxyl groups on the surface with mild acidity, physisorbed CO molecules, and CO bonded to  $\text{Ce}^{3+}$  sites, respectively, which are in close agreement with earlier data.<sup>[53]</sup> These data further indicate the existence of unsaturated coordination sites around  $\text{Ce}^{4+}$  in UiO-66(Ce) and are in agreement with the Raman spectra.

After confirming the structural formation of UiO-66(Ce) and the existence of unsaturated coordination sites around  $\text{Ce}^{4+}$ , the catalytic performance of this solid was examined in the Friedel-Crafts alkylation reaction between  $\beta$ -nitrostyrene and indole as model substrates. The results obtained are displayed in Table 1. A blank control experiment in the absence of UiO-66(Ce) solid showed no product formation at 80°C after 24 hr. In contrast, the precursors for the synthesis of UiO-66(Ce) were employed as catalysts for this reaction under identical conditions and 20% yield was observed for CAN while no yield was formed with the BDC linker. Furthermore, the use of n- $\text{CeO}_2$  provided 19% yield of the product under similar conditions. The reaction was also screened with various solvents (toluene, chloroform, ethanol,

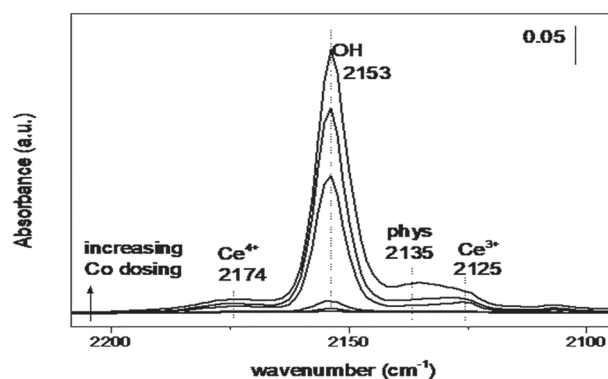


**FIGURE 7** *In situ* CO adsorption over UiO-66(Ce)

acetonitrile, dichloromethane, and dichloroethane [DCE], and the maximum yield was achieved with DCE as solvent at 80°C after 24 hr. Interestingly, UiO-66(Ce) furnished 91% yield of the desired product with 2 ml of DCE as solvent while the yield was further increased to 98% in a minimal amount of DCE (0.2 ml) at 80°C. Under these conditions, a control experiment was performed in the absence of catalyst and 13% yield observed, suggesting the crucial role of UiO-66(Ce) in promoting this reaction. Figure 8 shows the temporal profile in the evolution of yield as a function of time for CAN, n-CeO<sub>2</sub>, and UiO-66(Ce) as catalysts. This reaction was also optimized with respect to temperature and catalyst loading. The product yield was significantly reduced on decreasing the reaction temperature. The product yields were 63% and 50% at 70 and 60°C, respectively, under similar conditions. Similar behavior was also noticed with respect to the catalyst dosage, and the product yield was considerably affected on decreasing the loading. The observed results are shown in Figure 9. These results indicate that the population of Lewis acid sites decreased when the catalyst loading is reduced, thus hampering the reaction rate. In order to demonstrate the effective involvement of Lewis acid sites arising due to the participation of Ce<sup>4+</sup> in UiO-66(Ce) in this reaction, a control experiment was performed with pyridine as catalyst poison under optimized reaction conditions. The product yield was significantly reduced to 5% after 24 hr and this quenching in the reaction rate is due to the poisoning of Lewis acid sites available in the framework of UiO-66(Ce) through strong interaction with nitrogen by pyridine. Hence, the reactants are not able to coordinate with these sites, thus rendering poor yield in the presence of pyridine.

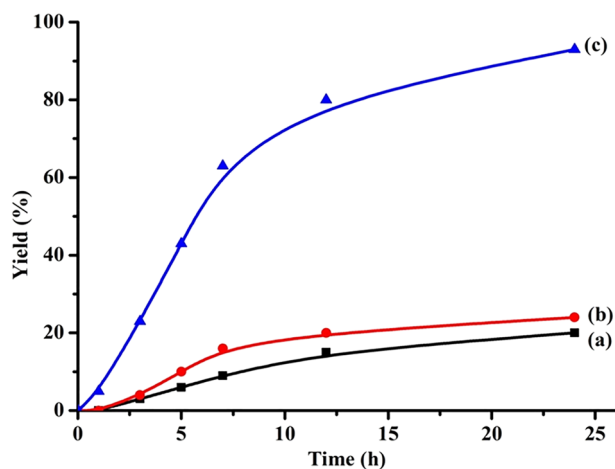


**FIGURE 8** Time-yield plots for the Friedel-Crafts alkylation reaction between indole and  $\beta$ -nitrostyrene using (a) n-CeO<sub>2</sub>, (b) CAN, and (c) UiO-66(Ce) as catalyst

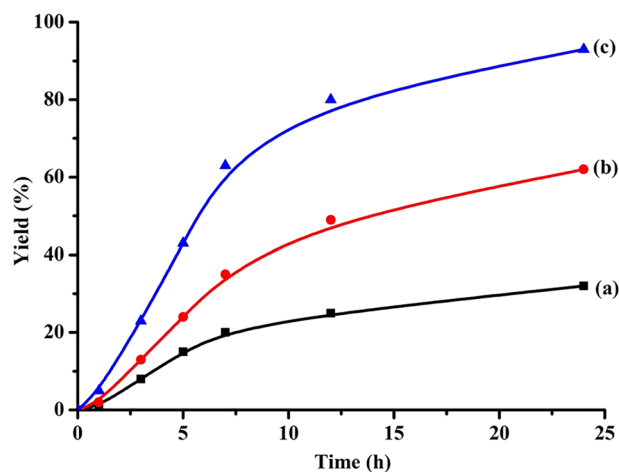


**FIGURE 9** Time-yield plots for the Friedel-Crafts alkylation reaction between indole and  $\beta$ -nitrostyrene using (a) 5 mg, (b) 15 mg, and (c) 25 mg of UiO-66(Ce)

One important experiment in heterogeneous catalysis is to confirm the heterogeneity of the reaction. Hence, the leaching test (hot filtration test) was performed using DCE as solvent at 80°C as the optimized conditions. The Friedel-Crafts alkylation reaction between these reactants was initiated and the solid catalyst was removed after 3 hr from the reaction mixture through syringe filtration at the reaction temperature. Later, the reaction mixture in the absence of solid catalyst was continued up to 24 hr and the progress of the reaction was monitored by GC. Comparison of the kinetic profile with and without solid catalyst indicates that the reaction progress stops when the catalyst is removed from the reaction mixture (Figure 10). These catalytic data clearly prove that the reaction is

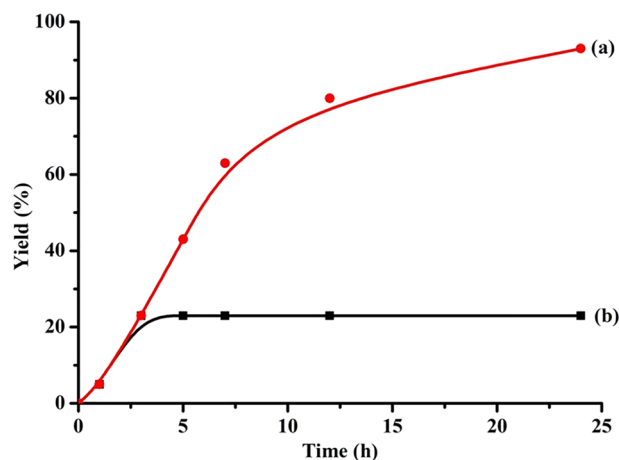


**FIGURE 10** Time-yield plots for the Friedel-Crafts alkylation reaction (a) in the presence of UiO-66(Ce) and (b) on filtration of UiO-66(Ce) solid after 3 hr and the reaction mixture stirred without catalyst under identical conditions

exclusively promoted by the Lewis acids present in UiO-66(Ce) and no  $\text{Ce}^{4+}$  ions are leached to the solution. Therefore, UiO-66(Ce) behaves as a heterogeneous solid under these reaction conditions. Furthermore, the catalyst stability was also confirmed by performing a reusability test in consecutive cycles. As shown in Figure 11, UiO-66(Ce) retained its catalytic activity up to four cycles without any reduction in its yield. This is more proof for the claim that the active sites in the solid are not leached or poisoned during these tests, thus showing similar activity in four cycles.

After ascertaining its robust stability from the leaching and reusability tests, the catalytic performance of UiO-66(Ce) was compared with other related Lewis acid MOFs commonly reported for other organic reactions under identical conditions. The observed catalytic data are shown in Figure 12. The activity of UiO-66(Ce) was much better than that of a series of catalysts, ZIF-8(Zn), MIL-101(Cr), ZIF-67(Co), MIL-101(Fe), and UiO-66(Zr), tested under similar conditions. The enhanced activity of UiO-66(Ce) compared to these catalysts is attributed to the high density of Lewis acid sites, easy accessibility by reactants, and the nature of the metal ion. Interestingly, the activity of UiO-66(Ce) shows two-fold higher activity than its analogous catalyst UiO-66(Zr) and this distinct activity difference is due to their Lewis acid behavior.<sup>[54]</sup>

The catalytic activity of a MOF in many organic reactions involving oxygen-containing compounds is often affected by the oxophilicity of the metal ion constituted within the MOF framework.<sup>[55–57]</sup> The interaction of Lewis acid sites with the oxygen atoms from the substrates is the key step in reducing the energy barrier in electrophilic C=C double bond of  $\beta$ -nitrostyrene to favor nucleophilic

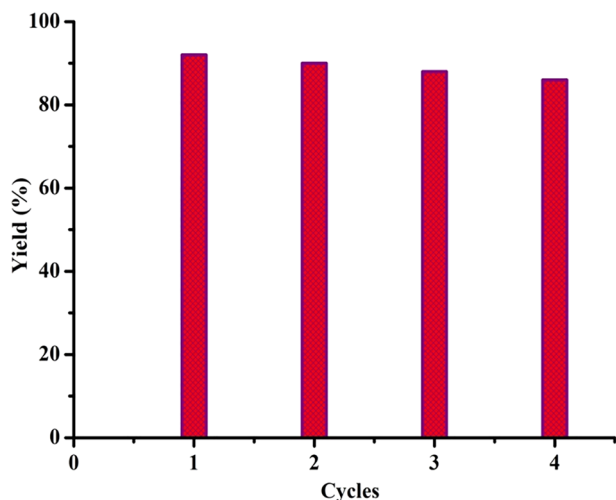


**FIGURE 11** Reusability data for the Friedel-Crafts alkylation reaction using UiO-66(Ce) as solid Lewis acid catalyst

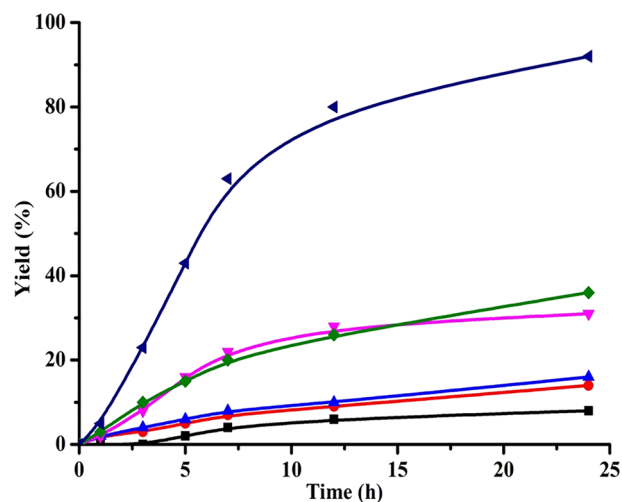


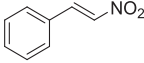
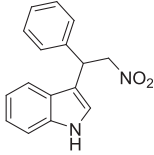
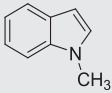
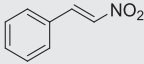
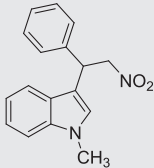
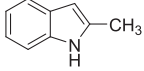
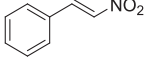
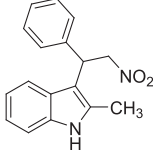
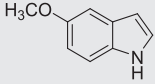
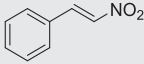
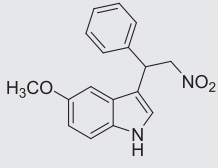
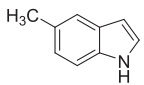
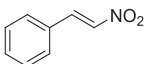
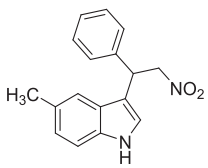
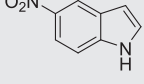
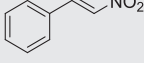
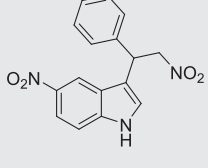
**FIGURE 12** Time-yield plots for the Friedel-Crafts alkylation reaction using (○) ZIF-8(Zn), (□) MIL-101(Cr), (△) ZIF-67(Co), (◇) MIL-101(Fe), (◆) UiO-66(Zr), and (◀) UiO-66(Ce)

attack. Hence, it is expected that those MOFs with metal ions having higher oxophilicity exhibit enhanced activity. Furthermore, the oxophilicities of Ce in UiO-66(Ce) and Zr in UiO-66(Zr) MOFs were 0.9 and 0.6, respectively, as revealed by density functional theory.<sup>[54]</sup> These results support the catalytic data observed in this study, thus suggesting the superior performance of UiO-66(Ce) although it has identical topology to UiO-66(Zr).<sup>[54,58]</sup>

Considering the stability and structural integrity of UiO-66(Ce) in this reaction under optimized reaction conditions, the scope of UiO-66(Ce) was screened with other indole derivatives. The results are displayed in Table 2. The Friedel-Crafts alkylation reaction between indole and  $\beta$ -nitrostyrene in the presence of UiO-66(Ce) afforded 98% yield at 80°C after 24 hr. The reaction between *N*-methylindole and  $\beta$ -nitrostyrene with UiO-66(Ce) showed 92% yield under similar conditions. Furthermore, 2-methyl-, 5-methoxy-, and 5-methylindoles reacted with  $\beta$ -nitrostyrene in the presence of UiO-66(Ce) to give 97%, 96%, and 95% yields, respectively. Unfortunately, the reaction of 5-nitroindole with  $\beta$ -nitrostyrene did not give any product under similar conditions. On other hand, 5-bromo and 5-chloroindoles efficiently reacted with  $\beta$ -nitrostyrene to afford higher yields of 90% and 92%, respectively. Besides indole, other nucleophiles, pyrrole and *N,N*-dimethylaniline, were also reacted with  $\beta$ -nitrostyrene to give 97% and 17% yields, respectively, under identical conditions. In general, the catalytic activity of UiO-66(Ce) was slightly higher in a minimal amount of DCE than in a large excess and this may be due to the steric crowd provided by chlorine atoms.

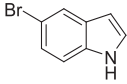
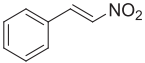
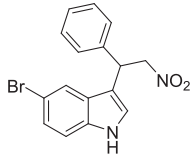
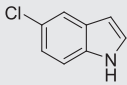
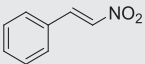
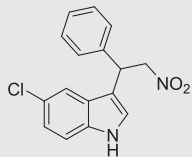
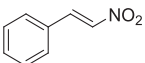
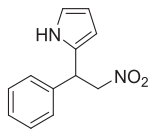
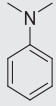
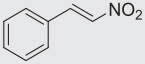
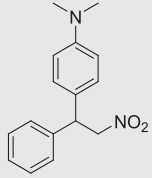
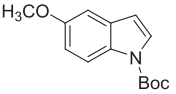
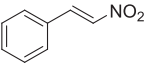
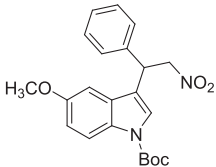
In order to address the location where the catalytic reaction occurs, a control experiment was performed using

**TABLE 2** Friedel–Crafts alkylation reaction of indoles with  $\beta$ -nitrostyrene using UiO-66(Ce) as a solid Lewis acid catalyst<sup>a</sup>

Entry	Indole	$\beta$ -nitrostyrene	Product	Yield <sup>b</sup> (%)	TON <sup>d</sup>
1				91 (98) <sup>c</sup>	20.8
2				82 (92) <sup>c</sup>	19.5
3				88 (97) <sup>c</sup>	20.6
4				85 (96) <sup>c</sup>	20.4
5				86 (95) <sup>c</sup>	20.2
6				–	0

(Continues)

TABLE 2 (Continued)

Entry	Indole	$\beta$ -nitrostyrene	Product	Yield <sup>b</sup> (%)	TON <sup>d</sup>
7				75 (90) <sup>c</sup>	19.1
8				77 (92) <sup>c</sup>	19.5
9				92 (97) <sup>c</sup>	20.6
10				11 (17) <sup>c</sup>	3.6
11				–	–

<sup>a</sup>Reaction conditions: indole (0.25 mmol),  $\beta$ -nitrostyrene (0.25 mmol), DCE (2 ml), UiO-66(Ce) (25 mg), 80°C, 24 hr.

<sup>b</sup>Yield was determined by GC.

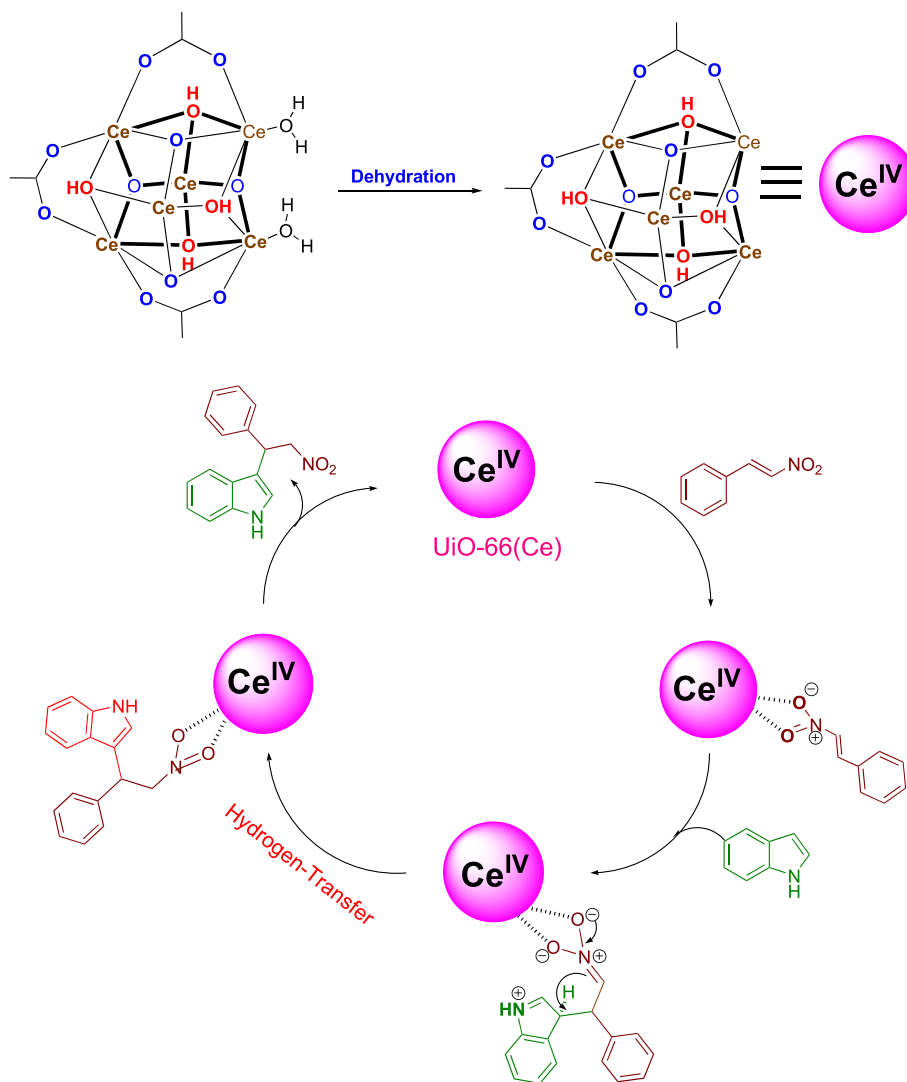
<sup>c</sup>Indole (0.25 mmol),  $\beta$ -nitrostyrene (0.25 mmol), DCE (0.2 ml), UiO-66(Ce) (25 mg), 80°C, 24 hr. Values in parentheses indicate the yield obtained under conditions "c".

<sup>d</sup>TON, turnover number: (mmol of product formed)/(mmol of uncoordinated cerium) under the reaction conditions in footnote c. The uncoordinated cerium in 25 mg of UiO-66(Ce) was 0.0235 mmol.

UiO-66(Ce) as solid acid catalyst for the reaction between N-Boc (tert-butoxycarbonyl) protected 5-methoxyindole and  $\beta$ -nitrostyrene under optimized reaction conditions, as shown in Table 2. The observed catalytic results indicated the absence of the desired product (Supporting Information Figure S28), thus indicating the diffusion limitation experienced by N-Boc-protected 5-methoxyindole in reaching the active site (Table 2, entry 11). In contrast,

the reaction of 5-methoxyindole with  $\beta$ -nitrostyrene afforded the expected product in 85% yield (Table 2, entry 4). Hence, these results prove that the reaction occurs mostly within the pores of UiO-66(Ce). The BET surface area and the micropore volume of UiO-66(Ce) were measured to be 1282 m<sup>2</sup>/g and 0.50 cm<sup>3</sup>/g, respectively, due to the presence of missing linkers,<sup>[26]</sup> thus allowing the reactants to penetrate without any diffusion restriction.

**SCHEME 2** A plausible mechanism for the Friedel–Crafts alkylation of indole with  $\beta$ -nitrostyrene catalyzed by UiO-66(Ce) as a solid Lewis acid catalyst



A plausible mechanism is proposed for the Friedel–Crafts alkylation reaction between indole and  $\beta$ -nitrostyrene (Scheme 2) using UiO-66(Ce) as a solid Lewis acid catalyst. As shown here, the coordinatively unsaturated vacant sites around Ce(IV) behave as Lewis acidic sites with high oxophilicity, thus readily interacting with  $\beta$ -nitrostyrene through an oxygen atom.<sup>[59]</sup> Furthermore, this interaction reduces the energy barrier in the electrophilic C=C double bond of  $\beta$ -nitrostyrene, thus favoring nucleophilic attack. Later, indole attacks  $\beta$ -nitrostyrene through C<sub>3</sub> to afford the expected Friedel–Crafts alkylation product.

## 4 | CONCLUSIONS

The applications of UiO-66(Ce) are greatly expanding due to its unique structural and chemical properties. Although the photocatalytic application of UiO-66(Ce) has been explored in recent years, no attempts have been made to expand the catalytic application of

this solid. This work has clearly shown that the catalytic activity of a MOF can be efficiently tuned by the oxophilicity of a metal ion under identical structural features and experimental conditions. The observed catalytic data revealed that the activity of UiO-66(Ce) is much higher than that of UiO-66(Zr) in the Friedel–Crafts alkylation reaction between  $\beta$ -nitrostyrene and indole under identical conditions. This enhanced activity of UiO-66(Ce) is due to its higher oxophilicity. Furthermore, UiO-66(Ce) showed almost similar catalytic activity up to four cycles with no decay in activity. The leaching test also supports the stability of this solid under these experimental conditions. This catalyst exhibits wider substrate scope, leading to the formation of broad heterocyclic compounds with higher yields.

## ACKNOWLEDGMENTS

AD thanks the University Grants Commission, New Delhi, for the award of an Assistant Professorship under its Faculty Recharge Programme. AD also thanks the

Science and Engineering Research Board, Department of Science and Technology, India, for financial support through Extra Mural Research Funding (EMR/2016/006500).

## CONFLICT OF INTEREST

There are no conflicts of interest to declare.

## ORCID

Amarajothi Dhakshinamoorthy  <https://orcid.org/0000-0003-0991-6608>

## REFERENCES

- [1] S. Chaemchuen, N. A. Kabir, K. Zhou, F. Verpoort, *Chem. Soc. Rev.* **2013**, *42*, 9304.
- [2] D. Farrusseng, *Metal-Organic Frameworks*, Wiley-VCH, Weinheim **2011**.
- [3] D. J. Tranchemontagne, J. L. Mendoza-Cortes, M. O'Keeffe, O. M. Yaghi, *Chem. Soc. Rev.* **2009**, *38*, 1257.
- [4] O. M. Yaghi, M. O'Keeffe, N. W. Ockwig, H. K. Chae, M. Eddaoudi, J. Kim, *Nature* **2003**, *423*, 705.
- [5] S. Ma, H.-C. Zhou, *Chem Commun* **2010**, *46*, 44.
- [6] J.-R. Li, J. Sculley, H.-C. Zhou, *Chem. Rev.* **2012**, *112*, 869.
- [7] A. Dhakshinamoorthy, A. M. Asiri, H. Garcia, *Adv. Mater.* **2019**, *31*, 1900617.
- [8] A. Dhakshinamoorthy, Z. Li, H. Garcia, *Chem. Soc. Rev.* **2018**, *47*, 8134.
- [9] B. Solomon, T. L. Church, D. M. D'Alessandro, *CrystEngComm* **2017**, *19*, 4049.
- [10] M.-X. Wu, Y.-W. Yang, *Adv. Mater.* **2017**, *29*, 1606134.
- [11] M. Yoon, K. Suh, S. Natarajan, K. Kim, *Angew Chem Int Ed* **2013**, *52*, 2688.
- [12] A. Santiago-Portillo, S. Navalón, M. Álvaro, H. García, *J. Catal.* **2018**, *365*, 450.
- [13] H. García, S. Navalón, *Wiley-VCH* **2018**, *1*.
- [14] C. Vallés-García, M. Cabrero-Antonino, S. Navalón, M. Álvaro, A. Dhakshinamoorthy, H. García, *J. Colloid Interface, J Colloid Int Sci* **2020**, *560*, 885.
- [15] M. Giménez-Marqués, A. Santiago-Portillo, S. Navalón, M. Álvaro, V. Briois, F. Nouar, H. Garcia, C. Serre, *J. Mater. Chem. A* **2019**, *7*, 20285.
- [16] A. Santiago-Portillo, S. Navalón, P. Concepción, M. Álvaro, H. García, *ChemCatChem* **2017**, *9*, 2506.
- [17] J. F. Blandez, A. Santiago-Portillo, S. Navalón, M. Giménez-Marqués, M. Alvaro, P. Horcajada, H. García, *J. Mol. Catal. A: Chem.* **2016**, *425*, 332.
- [18] J. H. Cavka, S. Jakobsen, U. Olsbye, N. Guillou, C. Lamberti, S. Bordiga, K. P. Lillerud, *J. Am. Chem. Soc.* **2008**, *130*, 13850.
- [19] A. Dhakshinamoorthy, A. Santiago-Portillo, A. M. Asiri, H. Garcia, *ChemCatChem* **2019**, *11*, 899.
- [20] F. Ragon, P. Horcajada, H. Chevreau, Y. K. Hwang, U. H. Lee, S. R. Miller, T. Devic, J.-S. Chang, C. Serre, *Inorg. Chem.* **2014**, *53*, 2491.
- [21] C. Gomes Silva, I. Luz, F. X. L. I. Xamena, A. Corma, H. Garcia, *Chem. – Eur. J.* **2010**, *16*, 11133.
- [22] F. Vermoortele, B. Bueken, G. Le, B. Bars, V. de Voorde, M. Vandichel, K. Houthoofd, A. Vimont, M. Daturi, M. Waroquier, V. Van Speybroeck, C. Kirschhock, D. E. De Vos, *J. Am. Chem. Soc.* **2013**, *135*, 11465.
- [23] C. Falaise, C. Volkringer, J.-F. Vigier, N. Henry, A. Beaurain, T. Loiseau, *Chem. – Eur. J.* **2013**, *19*, 5324.
- [24] E. Jakobsen, D. Gianolio, D. S. Wragg, M. H. Nilsen, H. Emerich, S. Bordiga, C. Lamberti, U. Olsbye, M. Tilset, K. P. Lillerud, *Phys. Rev. B: Condens. Matter Mater. Phys.* **2012**, *86*, 125429.
- [25] C. Falaise, J. S. Charles, C. Volkringer, T. Loiseau, *Inorg. Chem.* **2015**, *54*, 2235.
- [26] M. Lammert, M. T. Wharmby, S. Smolders, B. Bueken, A. Lieb, K. A. Lomachenko, D. E. De Vos, N. Stock, *Chem Commun* **2015**, *51*, 12578.
- [27] A. Buragohain, S. Biswas, *CrystEngComm* **2016**, *18*, 4374.
- [28] M. Stawowy, M. Róziewicz, E. Szczepanska, J. Silvestre-Albero, M. Zawadzki, M. Musioł, R. Łuzny, J. Kaczmarczyk, J. Trawczynski, A. Łamacz, *Catalysts* **2019**, *9*, 309.
- [29] R. Dalapati, B. Sakthivel, A. Dhakshinamoorthy, A. Buragohain, A. Bhunaia, C. Janiak, S. Biswas, *CrystEngComm* **2016**, *18*, 7855.
- [30] M. Lammert, C. Glißmann, N. Stock, *Dalton Trans* **2017**, *46*, 2425.
- [31] M. Lammert, H. Reinsch, C. A. Murray, M. T. Wharmby, H. Terraschke, N. Stock, *Dalton Trans* **2016**, *45*, 18822.
- [32] S. Smolders, A. Struyf, H. Reinsch, B. Bueken, T. Rhauderwiek, L. Mintrop, P. Kurz, N. Stock, D. E. De Vos, *Chem Commun* **2018**, *54*, 876.
- [33] Y. Zhang, X. Zeng, X. Jiang, H. Chen, Z. Long, *Microchem. J.* **2019**, *149*, 103967.
- [34] J. Yu, J. Yu, Z. Wei, X. Guo, H. Mao, D. Mao, *Catal. Lett.* **2019**, *149*, 496.
- [35] X.-P. Wu, L. Gagliardi, D. G. Truhlar, *J. Am. Chem. Soc.* **2018**, *140*, 7904.
- [36] Z. Yang, X. Xu, X. Liang, C. Lei, L. Gao, R. Hao, D. Lu, Z. Lei, *Appl. Surf. Sci.* **2017**, *420*, 276.
- [37] X.-P. Wu, L. Gagliardi, D. G. Truhlar, *J Chem Phys* **2019**, *150*, 041701.
- [38] A. Lin, A. A. Ibrahim, P. Arab, H. M. El-Kaderi, M. S. El-Shall, *ACS Appl. Mater. Interfaces* **2017**, *9*, 17961.
- [39] Y. Zhang, H. Chen, Y. Pan, X. Zeng, X. Jiang, Z. Long, X. Hou, *Chem Commun* **2019**, *55*, 13959.
- [40] G.-P. Lu, X. Li, L. Zhong, S. Li, F. Chen, *Green Chem.* **2019**, *21*, 5386.
- [41] R. Dalapati, B. Sakthivel, M. K. Ghosalya, A. Dhakshinamoorthy, S. Biswas, *CrystEngComm* **2017**, *19*, 5915.
- [42] V. Sridharan, J. C. Menendez, *Chem. Rev.* **2010**, *110*, 3805.
- [43] S. Lancianesi, A. Palmieri, M. Petrini, *Chem. Rev.* **2014**, *114*, 7108.
- [44] A. Z. Halimehjani, M. V. Farvardin, H. P. Zanussi, M. A. Ranjbari, M. Fattahi, *J. Mol. Catal. A: Chem.* **2014**, *381*, 21.
- [45] G. A. Olah, R. Khrisnamurti, G. K. S. Prakash (Eds), *C. O. Synthesis*, 1st ed. Vol. 3, Pergamon, New York **1991** 293.
- [46] E. K. Goharshadi, S. Samiee, P. Nancarrow, *J. Colloid Interface, J Colloid Int Sci* **2011**, *356*, 473.
- [47] N. Anbu, C. Vijayan, A. Dhakshinamoorthy, *ChemistrySelect* **2019**, *4*, 1379.
- [48] Z. Wang, Z. Quan, J. Lin, *Inorg. Chem.* **2007**, *46*, 5237.

- [49] F. Wang, S. He, H. Chen, B. Wang, L. Zheng, M. Wei, *J. Am. Chem. Soc.* **2016**, *138*, 6298.
- [50] G. C. Shearer, S. Chavan, J. Ethiray, J. G. Vitillo, S. Svelle, U. Olsbye, C. Lamberti, S. Bordiga, K. P. Lillerud, *Chem. Mater.* **2014**, *26*, 4068.
- [51] L. Valenzano, B. Civalieri, S. Chavan, S. Bordiga, M. H. Nilsen, S. Jakobsen, K. P. Lillerud, C. Lamberti, *Chem. Mater.* **2011**, *23*, 1700.
- [52] H. Wu, Y. S. Chua, V. Krungleviciute, M. Tyagi, P. Chen, T. Yildirim, W. Zhou, *J. Am. Chem. Soc.* **2013**, *135*, 10525.
- [53] C. Binet, M. Daturi, J.-C. Lavalley, *Catal. Today* **1999**, *50*, 207.
- [54] K. P. Kepp, *Inorg. Chem.* **2016**, *55*, 9461.
- [55] X. Li, Q. Deng, L. Zhang, J. Wang, R. Wang, Z. Zeng, S. Deng, *Appl Catal a Gen* **2019**, *575*, 152.
- [56] O. A. Kholdeeva, I. Y. Skobelev, I. D. Ivanchikov, K. A. Kovalenko, V. P. Fedin, A. B. Sorokin, *Catal. Today* **2014**, *238*, 54.
- [57] M. Opansenko, A. Dhakshinamoorthy, Y. K. Hwang, J.-S. Chang, H. Garcia, J. Čejka, *ChemSusChem* **2013**, *6*, 865.
- [58] T. Islamoglu, A. Atilgan, S.-Y. Moon, G. W. Peterson, J. B. Decoste, M. Hall, J. T. Hupp, O. K. Farha, *Chem. Mater.* **2017**, *29*, 2672.
- [59] K. Tanaka, K. Sakuragi, H. Ozaki, Y. Takada, *Chem Commun* **2018**, *54*, 6328.

## SUPPORTING INFORMATION

Additional supporting information may be found online in the Supporting Information section at the end of this article.

**How to cite this article:** Nagarjun N, Concepcion P, Dhakshinamoorthy A. Influence of oxophilic behavior of UiO-66(Ce) metal-organic framework with superior catalytic performance in Friedel-Crafts alkylation reaction. *Appl Organometal Chem.* 2020;e5578. <https://doi.org/10.1002/aoc.5578>